CHARACTERIZATION AND MULTISCALE MODELING OF LIQUID CRYSTALLINE MATERIALS AND THEIR BIOLOGICAL ANALOGUES

Dana Grecov

ABSTRACT. Nematic liquid crystals are textured, anisotropic, viscoelastic materials. The remarkable rheological properties of viscoelastic materials are governed by the flow-induced evolution of molecular configuration. Analogues to liquid crystal flow processes occur in the supramolecular self-assembly processes of living biological tissues. A good understanding of the relationships between rheological properties and microstructural evolution of liquid crystals can provide insights towards a predictive rheology of complex biomaterials. Silk fibers and other biomaterials have embedded the natural structure that is more compatible with other biomaterials, and hence biomedical materials produced from biological inspired microstructures will also display enhanced compatibilities.

2000 *Mathematics Subject Classification*: 76M20, 76D05.

1. Introduction

The orientational order of liquid crystal polymers offers a unique pathway to create new nano- and microstructures with unique optical, electromagnetic, and mechanical properties. Nematic liquid crystals are textured, anisotropic, viscoelastic materials. The remarkable rheological properties of viscoelastic materials are governed by the flow-induced evolution of molecular configurations. Furthermore, the frozen-in microstructure that develops in processing flows dictates the physical properties of the final product. Their mechanical behavior is greatly influenced by the presence of textures, or spatial distribution of topological defects. Shear-induced nucleation and annihilation of topological defects in nematic liquid crystals is a phenomenon of both scientific interest and practical importance.

The objective of this paper is to present a multiscale theory and simulation for hydrodynamic texture formation in liquid crystalline materials, useful to the creation of synthetic material structures and the biomimetics of natural fibers. Fundamental principles for control and optimization of structures in liquid crystalline materials are provided. Analogues to liquid crystal flow processes occur in the supramolecular self-assembly processes of living biological tissues. A good understanding of the relationships between rheological properties and microstructural evolution of liquid crystals can provide insights towards a predictive rheology of complex biomaterials.

Silk fibers and other biomaterials have embedded the natural structure that is more compatible with other biomaterials, and hence biomedical materials produced from biological inspired microstructures will also display enhanced compatibilities. Substantial contributions have already made to understanding of the properties and material processing of liquid crystal biomaterials liquid crystal-like.

2. Theory and governing equations

We present the Landau-de Gennes theory for nematic liquid crystals and the parametric equations used to describe liquid crystalline polymers texture formation. The theory is well suited to simulate texture formation since defects are non-singular solutions to the governing equations. In this paper we study a rectilinear simple start-up shear flow with Cartesian coordinates, as shown in figure 1. The lower plate is fixed and the upper plate starts moving at t=0 with a known constant velocity V; the plate separation is H. The z axis is coaxial with the vorticity axis and the shear plane is spanned by the x-y axes- figure 1.

The microstructure of thermotropic liquid crystal polymers is described conveniently in terms of a second order, symmetric and traceless tensor order parameter $\mathbf{Q}$ [1]:

$$\mathbf{Q} = \int (\mathbf{u}\mathbf{u} - \mathbf{I}/3) f d^2 r \tag{1}$$

where $\mathbf{u}$ is the unit vector normal to the rod-like molecules, I is second order unit tensor, and f is the orientation distribution function. The governing equations for liquid crystal flows follow from the dissipation function Δ:

$$\Delta = \mathbf{t}^s : \mathbf{A} + ckT\mathbf{H} \cdot \hat{\mathbf{Q}} \tag{2}$$
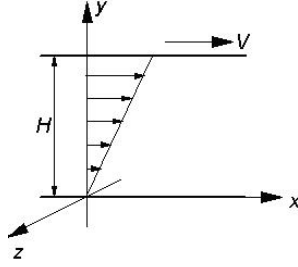
Figure 1: Definition of the flow geometry and coordinates system for simple shear flow. The lower plate is at rest and the upper plate moves in the x-direction with a constant velocity V. H is the gap separation

where $\mathbf{t}_s$ is the viscoelastic stress tensor, c is the concentration of molecules per unit volume, k the Boltzmann constant and T the absolute temperature, $\mathbf{A}$ is the symmetric traceless rate of deformation tensor, $\mathbf{H}$ is the molecular field, and $\hat{\mathbf{Q}}$ is the Jaumann derivative of the tensor order parameter, given by:

$$\hat{\mathbf{Q}} = \frac{\partial \mathbf{Q}}{\partial t} + (\mathbf{v} \cdot \nabla)\,\mathbf{Q} - \mathbf{W} \cdot \mathbf{Q} + \mathbf{Q} \cdot \mathbf{W} \tag{3}$$

$$\mathbf{A} = 1/2\left(\nabla \mathbf{v} + \nabla \mathbf{v}^T\right) \tag{4}$$

$$\mathbf{W} = 1/2\left(\nabla \mathbf{v} - \nabla \mathbf{v}^T\right) \tag{5}$$

$$(ckT) = -\left[\frac{\partial f}{\partial \mathbf{Q}} - \nabla \cdot \frac{\partial f}{\partial \nabla \mathbf{Q}}\right]^{[s]} \tag{6}$$

where f is the free energy density given in [2].

The dynamics of the tensor order parameter is given by the following sum of flow $\mathbf{F}$, short range $\mathbf{H}^{sr}$, and long range $\mathbf{H}^{lr}$ contributions [2]:

$$\hat{\mathbf{Q}} = \mathbf{F}\left(\mathbf{Q}, \nabla \mathbf{v}\right) + \mathbf{H}^{sr}\left(\mathbf{Q}, D_r\right) + \mathbf{H}^{lr}\left(\nabla \mathbf{Q}\right) \tag{7}$$

where D_r is the microstructure dependent rotational diffusivity.

3. COMPUTATIONAL METHODS

The model equations are a set of five coupled non-linear parabolic partial differential equations. The equations are solved using Galerkin Finite Elements for spatial discretization and a fourth order Runge-Kutta time adaptive method. Convergence and mesh-independence were established in all

293

cases using standard methods. Spatial discretization was judiciously selected taking into account the length scale of our model. The selected adaptive time integration scheme is able to efficiently take into account the stiffness that rises due to the disparity between the lenghtscales and between time scales. The boundary conditions for **Q** are:

$$\mathbf{Q}_s\left(y^* = 0\right) = \mathbf{Q}_s\left(y^* = 1\right) = S_{eq}\left(\mathbf{n}_s\mathbf{n}_s - \frac{\mathbf{I}}{3}\right) \tag{8}$$

$$\mathbf{n}_s = (0, 0, 1)) \tag{9}$$

$$S_{eq} = \frac{1}{4} + \frac{3}{4}\sqrt{1 - \frac{8}{3U}} \tag{10}$$

describing fixed director orientation along the vorticity axis , a uniaxial state with the scalar order parameter equal to its equilibrium value. The initial state is assumed to be uniaxial and at equilibrium. The initial orientation of the director is assumed to be random.

4. NUMERICAL RESULTS AND DISCUSSION

Previous work [3] has shown that as the shear rate (Ericksen number) increases, the Landau-deGennes theory predicts the existence of six stable steady state modes, as follows:

1. Homogeneous mode (H): the director is aligned everywhere along the vorticity axis (n_z=1).

2. Symmetric mode (S): the director reorients uniformly towards the shear plane, creating a symmetric twist angle profile. Since the reorientation has a unique sense (say clockwise) no twist wall appear at the center region.

3. Asymmetric mode (A): the re-orientation direction in the top half-layer is opposite to the bottom half-layer. The resulting director field exhibits a twist wall at the center of the gap, and two boundary layers at the bounding surfaces.

4. Defect lattice mode (DL): The number of re-orientation reversal increases with increasing shear rate, and the director filed display a finite number of twist inversion walls separated by a nearly constant distance.

The mode is spatially periodic and the wave-length is the wall-wall distance. Since the mode is periodic it is denoted defect lattice. In this mode no coarsening processes (i.e., annihilation) occur. If annihilation takes place periodicity is destroyed.

5. Defect gas mode (DG): in this mode annihilation processes set in and walls nucleate and react with other walls, with the bounding surfaces, and/or they pinch. Since coarsening is a random process it destroys periodicity and the mode is referred as a defect gas mode. The twist wall distance is a random variable.

6. Planar mode (P): At the highest shear rates, annihilation by pinching overcomes defect nucleation, and no twist walls remain at steady state. The resulting mode is planar and defect free.

It is found [3] that the texture transition cascade is remarkably consistent with the textural transition of sheared lyotropic tumbling nematic polymers [4]. Since the governing time scales at high shear rates are the flow time scale, all transient results are plotted as a function of strain . In the following we will present results for the last 3 modes.

Figure 2 shows computed gray scale visualizations of director component n_z ($0 \leq y^* \leq 1$) as a function of strain, corresponding to the three modes : a) symmetric mode- oriented domain (S), De=0.001; b) defect lattice mode (DL), De=0.05; c) defect gas mode (DG) mode, De=1.3; d) planar mode (P) De=1.5. Black represents in plane orientation (n_z =0) and light represents orientation along the vorticity (n_z=1) axis. The flow induced textural transformations considered in this paper are nucleation and annihilation of twist inversion walls. Twist walls arise whenever two equivalent director re-orientations under an external flow are possible.

Here they arise because the director is initially oriented along the vorticity and the director reorientation can follow two dissipatively and elastically equivalent paths towards the shear plane. Since twist walls represent localized elastic energy regions, the system will activate annihilation processes.

Thus textural transformations refer to wall nucleations and wall annihilations. The steady state texture of a liquid crystal is given by the balance of nucleation and coarsening processes. Coarsening events limit the lifetime of an inversion wall, and a texture can be viewed as a balance between birth-death events. Coarsening processes of inversion walls under shear can
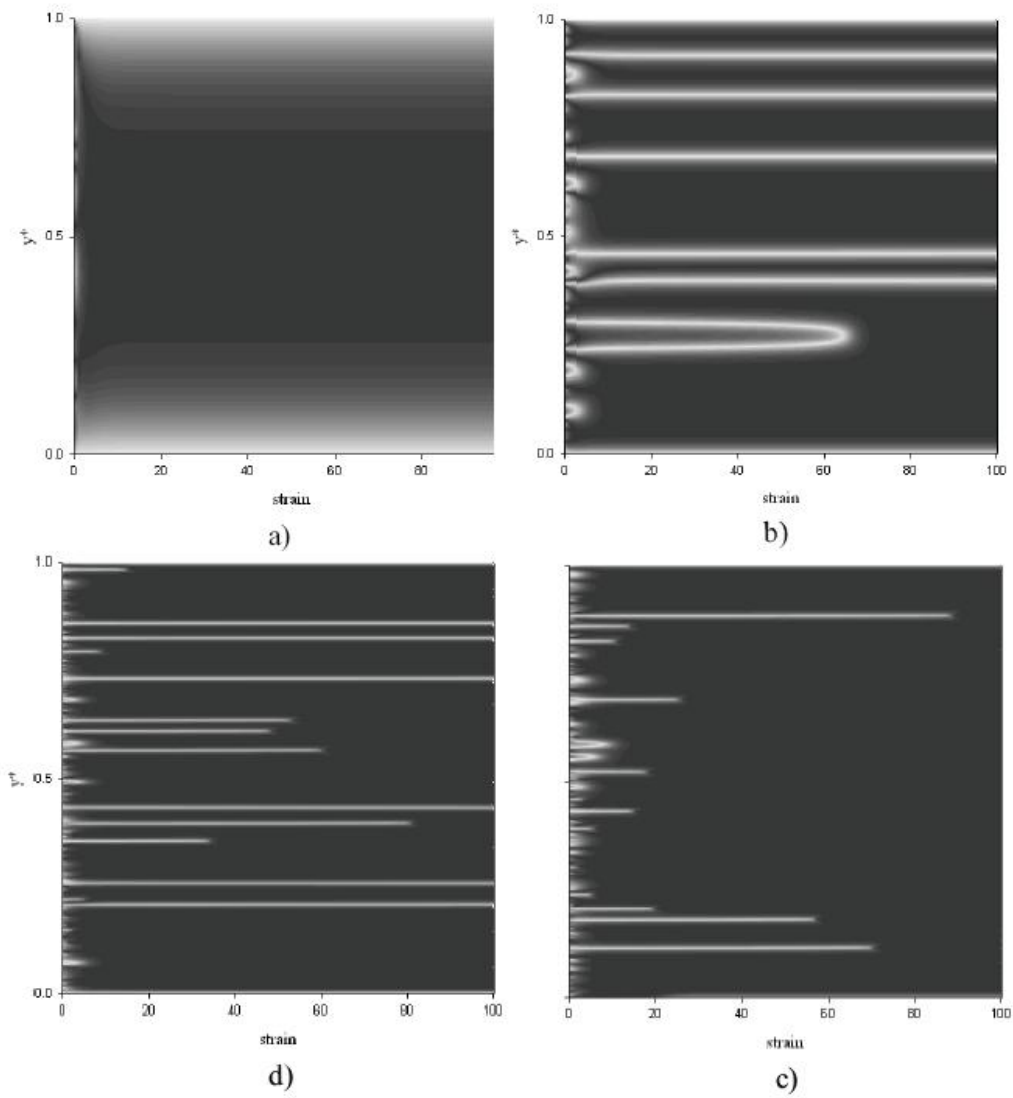
Figure 2: Computed gray scale visualization of director component n_z ($0 \leq y^* \leq 1$) as a function of strain: a) symmetric mode(H); b) defect lattice mode (DL); c) defect gas mode (DG); d) planar mode (P)

involve: (a) wall-bounding surface reaction, (b) wall-wall annihilation and (c) pinching [3].

Figure 3(a) shows a computed visualization of director component n_z $(0 \leq y^* \leq 1)$ as a function of strain for R=10^6, U=4, De=0.03, corresponding to wall-bounding surface interaction and wall-wall annihilation in the defect lattice mode.

a)   b)
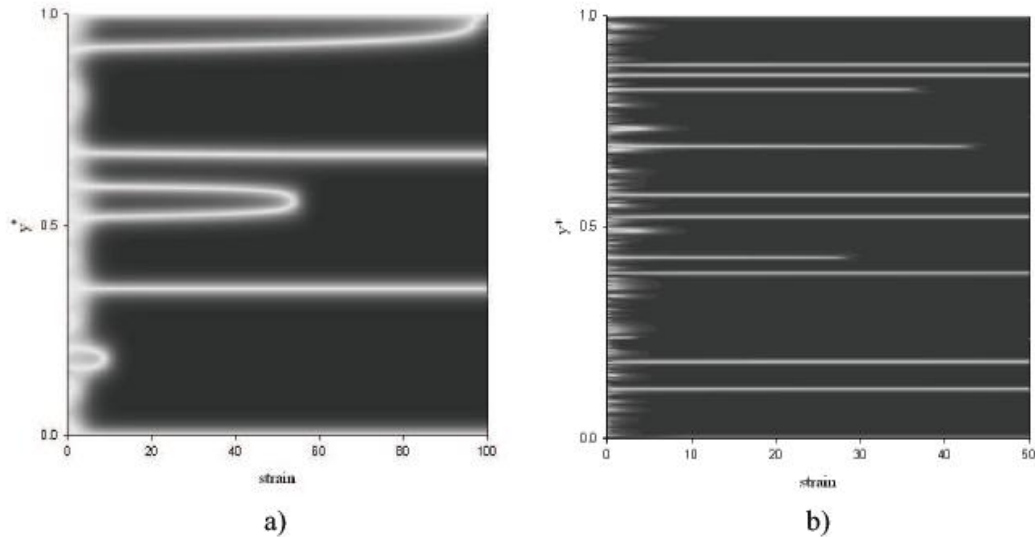
Figure 3: Computed visualization of director component n_z $(0 \leq y^* \leq 1)$ as a function of strain. Black represents in plane orientation $(n_z=0)$ and light orientation along the vorticity $(n_z=1)$: a) wall-bounding surface interaction and wall-wall interaction in defect lattice mode, De=0.03; c) wall pinching in planar mode, De=1.4.

Black represents in plane orientation (nz=0) and light orientation along the vorticity $(n_z =1)$. As strain increases one wall is absorbed by the bounding surface leaving behind a single wall in the bulk.

Figure 3(a) is a unique example of a defect-bounding surface interaction. As strain increases the walls annihilate leaving behind a planar director field. Figure 3(b) shows a computed visualization of director component nz $(0 \leq y^* \leq 1)$ as a function of strain for R=10^6, U=4, De=1.4, corresponding to wall pinching in the planar mode. Black represents in plane orientation $(n_z$

297

=0) and light orientation along the vorticity (n_z =1). As strain increases the walls pinch separately leaving behind a planar director field.

5. Conclusions

In summary, the presented multiscale theory and simulation of hydrodynamic meso and macrotexture formation is able to provide fundamental principles for control and optimization of structures in polymer-liquid crystal materials. Flow processes nucleate defects under the influence of velocity gradients. This paper shows that computational modeling of liquid crystal polymer materials offers an efficient pathway to discover new multiscale microstructures and provides science-based complex biomaterials and biological inspired microstructures liquid crystal analogues manufacturing principles.

References

[1] P.G. de Gennes and J. Prost ,The physics of Liquid Crystals, 2nd edn., Clarendon Press, Oxford,1993.

[2] D. Grecov and A.D. Rey, Theoretical and Computational Rheology for Discotic Nematic Liquid Crystals. Mol Cryst Liq Cryst. 391(1),2002, 57-94.

[3] D. Grecov and A.D. Rey, Shear-induced textural transitions in flow-aligning liquid crystal polymers, Phys. Rev. E, 68, 2003, 061704.

[4] G. Marrucci, Remarks on the viscosity of polymeric liquid crystals, In Mena B, Garcia-Rejon A, Rangel-Nafaile C, editors. Advances in Rheology, Vol. 1. Universidad National Autonoma De Mexico, Mexico, 1984.

Author:

Dana Grecov
Department of Mechanical Engineering
University of British Columbia
6250 Applied Science Lane, Vancouver, V6T 1Z4, Canada
email:*dgrecov@interchange.ubc.ca*